Land cover change as an additional forcing to explain the rainfall decline in the south west of Australia

B. Timbal[1] and J. M. Arblaster[2,3]

Received 1 December 2005; revised 21 February 2006; accepted 14 March 2006; published 15 April 2006.

[1] A fully coupled climate model forced with natural and anthropogenic atmospheric forcings is used to investigate the rainfall decline in the south west of Australia. Results are compared between experiments with two different land covers. We found that vegetation cover affects modelled rainfall in the region and enhances the model response to anthropogenic atmospheric forcings, which were found in a previous study to explain part of the observed rainfall decline. This result is observed directly in model rainfall and using a statistical downscaling technique which relates local rainfall to mean sea level pressure and large-scale rainfall. While the rainfall response to anthropogenic forcings is driven mostly by the changes in pressure, the land cover influences directly the modelled rainfall (large-scale and total) and thus indirectly the downscaled rainfall.
Citation: Timbal, B., and J. M. Arblaster (2006), Land cover change as an additional forcing to explain the rainfall decline in the south west of Australia, *Geophys. Res. Lett.*, *33*, L07717, doi:10.1029/2005GL025361.

1. Introduction

[2] A small area at the south west tip of the Australian continent (hereafter, SWA) enjoys a Mediterranean climate with winter rainfall from May to October (up to 1000 mm) and contrasts with a dry continent inland. A sharp drop in rainfall was observed in the 1960s and 1970s for the early part of the wet season (May to July). This decline ranges from 15 to 20 and affects the central and southern part of the region (*IOCI*, 2002).

[3] Studies, using observations [*Allan and Haylock*, 1993] and models [*Indian Ocean Climate Initiative Panel (IOCI)*, 2002] have shown that large-scale Mean Sea Level Pressure (MSLP) trends relate well to the rainfall decline. Statistical downscaling techniques [*Timbal*, 2004], using such linkages, are able to capture the rainfall trend. They have proven valuable tools to complement climate model based studies due to the small size of the region affected. However, the attribution of the decline has proven a difficult task. On the balance of the scientific evidence, *IOCI* [2002] suggested that natural variability, anthropogenic climate change and land clearance are all plausible causes of the decline, although land clearance was likely to be a secondary effect. Recent studies have shown that although multi-decadal variability is sufficient to explain this change [*Cai et al.*, 2005], the decline is consistent with General Circulation Model (GCM) simulations of a future climate under enhanced greenhouse concentrations [*Hope*, 2006]. *Timbal et al.* [2006, hereafter TI06], were able to show, using a downscaling technique applied to two ensembles of simulations of the 20th century, that the rainfall decline was unlikely to be due to natural external forcing of the climate system such as variability in solar input and volcanic eruptions. However, when these natural forcings were combined with additional man-made forcings (greenhouse gases, ozone and sulphate aerosols), the model was able to simulate the rainfall decline, although with only half the magnitude of the observed decline and with a progressive decline during the second half of the 20th century rather than an abrupt shift.

[4] The possibility that large-scale land clearance was a cause of the rainfall decline [*IOCI*, 2002] was tested by *Pitman et al.* [2004, hereafter PI04], following observational studies of the impact of land cover on local meteorology in SWA [*Lyons*, 2002]. The clearance of the land due to European settlement started in the early 19th century. An area of roughly 200,000 km^2 (half being native trees and the other half being shrubland) was replaced by grass and crops [*Australian Surveying and Land Information Group*, 1990]. This land clearance occurred by and large during the middle of the 20th century (1920 to 1980). *Williams* [2003] qualifies this clearing as "brutal" and estimates that by the 1990, at least 120,000 km^2 of original vegetation had been modified. PI04 were able to simulate a similar, but arguably, smaller, rainfall decline to that observed by reducing forest cover in perpetual July simulations, using Regional Climate Models (RCMs). The mechanism suggested by PI04 is that the land clearance reduces the roughness length, which then increases the low level wind, decreases the moisture convergence, and thus affects the rainfall. The present study aims at investigating land cover as an additional factor to complement TI06 findings and to test the mechanism described by PI04 in a different modelling framework.

2. Data and Method

[5] The Parallel Climate Model (PCM) developed at the National Center for Atmospheric Research (NCAR) with support from the Department of Energy [*Washington et al.*, 2000] is used here. The control comprises an ensemble of four experiments run over 1890 to 1999 with a full set of forcing (FF, hereafter): natural and anthropogenic [*Meehl et al.*, 2004]. The model has been integrated once more with a different vegetation cover, first for 400 years before reaching equilibrium and then during the 20th century with full

[1] Bureau of Meteorology Research Centre, Melbourne, Victoria, Australia.
[2] National Center for Atmospheric Research, Boulder, Colorado, USA.
[3] Also at Bureau of Meteorology Research Centre, Melbourne, Victoria, Australia.

0094-8276/06/2005GL025361$05.00

forcing (FFL hereafter). The purpose of this experiment was to test the impact of human land cover information from the IMAGE land surface database [*Alcamo*, 1994], on the original vegetation of the land surface model [*Bonan*, 1996]. The vegetation cover differs worldwide with noticeably large regional effects [*Feddema et al.*, 2005], which effectively cancel out to give a small global change. In FF, the nine grid boxes covering the area of interest (SWA) have a gradient of broadleaf evergreen tree from the southwest tip inland. In FFL, SWA has a cover of 80% grassland and 20% bare land with the exception of a single grid point at the tip of the continent classified as crop with 15% bare land. The land clearance implied between the two experiments is much larger than that observed: 240,000 km^2 of forest are removed as well as 550,000 km^2 of shrubland, roughly four time the observed clearance. It is expected that these vegetation types in FF and FFL will affect the hydrological cycle and surface energy partitioning worldwide [*Feddema et al.*, 2005]. Although not originally designed for this purpose, the changes from FF to FFL, at the scale of SWA, are consistent with PI04 land clearance experiments (albeit larger) and prove an opportunity to validate the mechanism described by PI04 within the broader context of large-scale changes occurring due to external atmospheric forcings. Although, the magnitude of the forcing will prevent us in quantifying the role of such mechanism in the observed rainfall decline. PI04 noted that surface roughness length (Z_o) was the critical surface change to contribute to the rainfall reduction, ahead of other surface properties. Z_o is strongly reduced in our experiments. It is worth noting that in our study we cannot differentiate between the role of reduced Z_o and other changes affecting the surface cover, at best, we will examine if our model reproduces the anomalies observed by PI04 which they attribute to changes in Z_o.

3. Impact of Modern Vegetation on Downscaled Rainfall Trends

[6] To exploit models ability to simulate large-scale fields reasonably well and circumvent errors in directly simulated rainfall, *Timbal* [2004] adapted a statistical downscaling model based on the idea of analogous situations to study SWA rainfall. It relies on Mean Sea Level Pressure (MSLP) and large-scale (or stratiform) rainfall to reproduce locally observed rainfall series. Applied to FF, which produces a shift of the high-pressure belt poleward in the second half of the 20th century, the technique simulates a rainfall decline (TI06). The downscaling provides a stronger decline than the direct rainfall from the model, although the downscaled rainfall decline is still only about half of the observed one. Here, the same statistical model as per TI06 (including the estimate of the uncertainties in the statistical linkage) is applied to FFL.

[7] Rainfall trends from the reconstructed series are nearly three times larger in FFL than in FF (Figures 1b and 1c). There is, however, overlap between the ranges of uncertainties for both model results, with the observed trends falling within this overlap (Figure 1a). The uncertainties are larger with FF as they reflect both the uncertainties arising from the ensemble simulations and the statistical linkage, which are always smaller. Results from FFL are based on a single model simulation and only

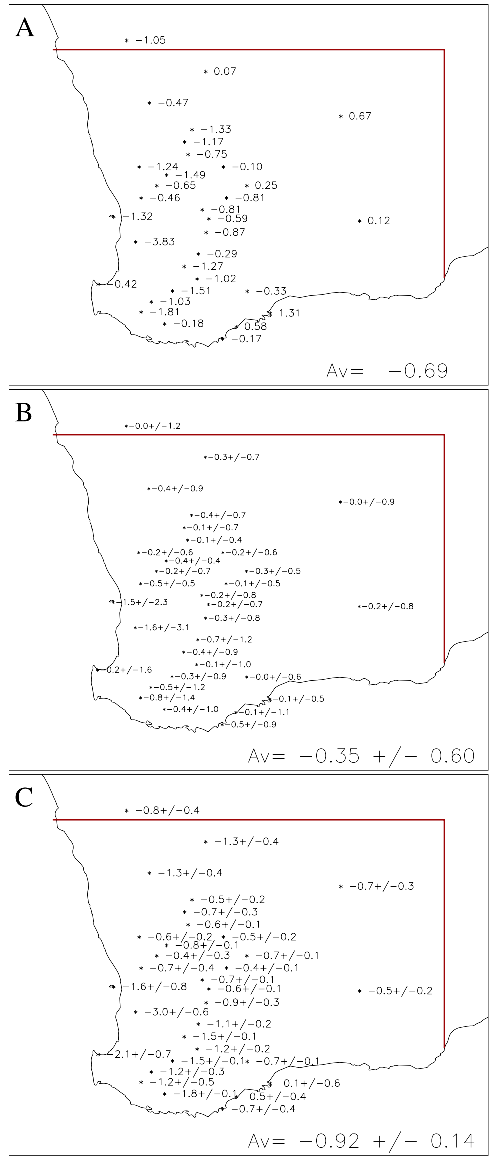

Figure 1. May-June-July rainfall decline from 1958 to 1998 at 32 stations in SWA expressed as a linear trend in mm.year^{-1}, for (a) observed series and statistically reconstructed series from (b) FF and (c) FFL, with uncertainties attached.

reflects the statistical linkage uncertainties. On face value, this result suggests that the enhancement of the rainfall decline is possibly due to local land cover change, as suggested by PI04. Alternatively, in the absence of an ensemble for FFL, it is not possible to rule out that the difference is due to randomly generated internal variability; it could also be remotely linked to global and not local vegetation changes. While the first hypothesis is difficult to discard, it is worth pointing that none of the FF member exhibits a signal as large as FFL, either from downscaled or direct model rainfall (Table 1). The second hypothesis is not supported by a range of studies (PI04) and the global analysis of FFL [*Feddema et al.*, 2005].

[8] The observed rainfall decline has a noticeable spatial pattern with largest values along the western escarpment.

Table 1. Spatial Average of the May-June-July Linear Rainfall Trends Obtained From the PCM Simulations Using Model Rainfall and the Downscaling Technique[a]

		Downscaling		
	Direct Model Rainfall	MSLP + LSR	MSLP	Obs.
FFL	−0.93	−0.92 ± 0.10	−0.31 ± 0.30	−0.69
FF	−0.17 ± 0.49	−0.35 ± 0.60	−0.38 ± 0.71	

[a]Rainfall trends include associated uncertainties; PCM simulations include experiment FFL and ensemble FF; the downscaling technique was done with one or two predictors; and the observed rainfall trend is provided.

Further inland, the rainfall decline decreases rapidly and reverses to a positive trend. This feature is not seen in statistically downscaled results; the FFL experiment does not improve the spatial pattern of the reconstructed rainfall decline in SWA but does produce a larger decrease across the entire domain.

4. Impact of Modern Vegetation on Large-Scale Predictors

[9] The statistical model relies on two large-scale predictors: MSLP and large-scale rainfall, a proxy for the moisture available in the atmosphere. Table 1 shows results from both direct model rainfall and with the statistical downscaling. Spatial averages of direct model rainfall are made comparable to downscaled rainfall using the nearest grid point to each station. The downscaling model was applied with both predictors combined and with MSLP alone. The rainfall trend is not as strong in FFL when using MSLP alone, weakening from −0.92 mm.year−1 to −0.31. The inclusion of large-scale rainfall makes little impact on the results in FF. Results are similar with direct model rainfall. This suggests that amongst the two predictors considered, MSLP determines rainfall response in FF, while the enhancement in FFL comes from large-scale rainfall. The high variability, and thus large uncertainties, in the FF ensemble is driven by different MSLP responses as seen in the uncertainty range while the model response for large-scale rainfall is extremely consistent across the FF ensemble: the uncertainty is slightly reduced when large-scale rainfall is used as an additional predictor (Table 1). It is also worth noting that in FFL (but not in FF), the rainfall response is clearly visible in the direct model rainfall.

[10] Linear trends fitted to large-scale rainfall (Figure 2) feature a broad area of increase across the northeast of Australia and an area of decline across SWA, in both FF and FFL. However, the position, the size and the magnitude of these anomalies differ between the two model results leading to opposite trends within the area (shown as a black box) used by the downscaling model. In FFL, the large-scale rainfall decrease is large in magnitude and extends inland (consistent with the downscaled results). It is worth noting that none of the individual simulations in the FF ensemble (not shown) exhibit similar patterns.

5. Mechanism to Explain the Modern Vegetation Impact

[11] The variables identified by PI04 to explain the impact of land clearance on rainfall are compared between

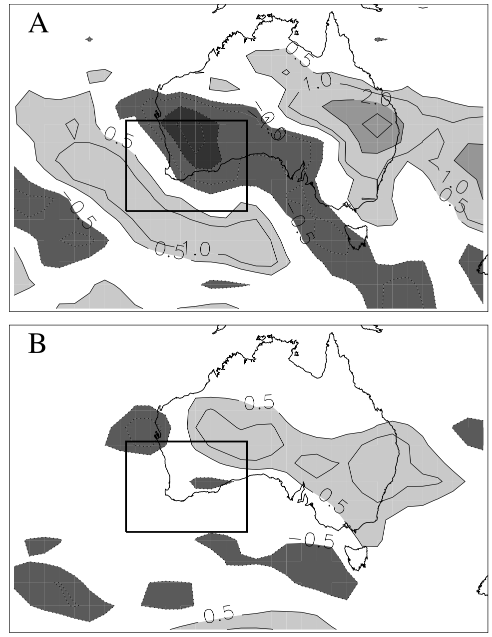

Figure 2. Maps of linear trends for large-sale rainfall (in tenth of mm d^{-1} over 41 years from 1958 to 1998) for (a) FFL and (b) FF.

FFL and a single simulation from the FF ensemble to ensure consistency. We chose the most similar simulation to the ensemble mean, however results are not sensitive to the simulation used. Results are averaged from May to July, over 41 years from 1958 to 1998, and analysed for the three lowest hybrid sigma levels from the model (992, 970 and 929 hPa) for wind speed, specific humidity and vertical velocity (Figures 3a–3c). Wind speed is larger in FFL along

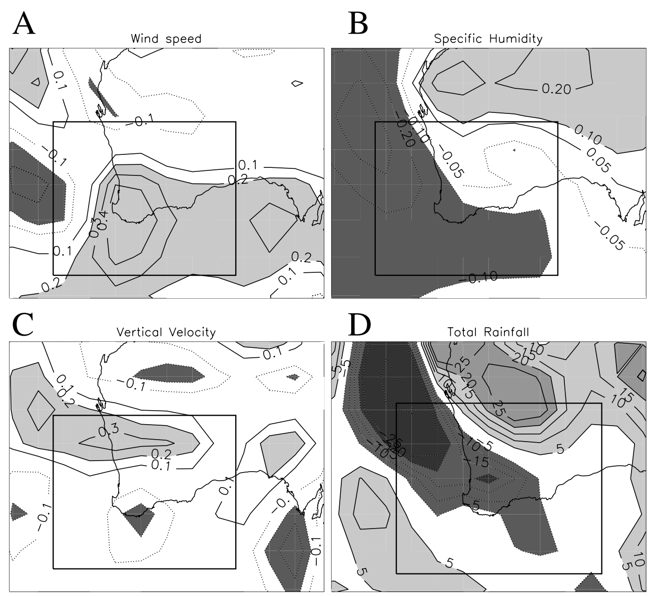

Figure 3. May-June-July differences between FFL and one experiment in FF, averaged from 1958 to 1998 across the three lowest model levels, for (a) Wind speed (in $m.s^{-1}$), (b) Specific Humidity (in $g.Kg^{-1}$) and (c) Vertical Velocity (in $10^{-2}.Pa.s^{-1}$); and for (d) total modelled rainfall (in mm).

the western coast of SWA, above the two grid boxes where high trees with Z_o = 2.6 m are replaced by low vegetation (crops and grass) with Z_o = 6 cm. The difference is largest at the lowest level and represents up to 10% of the long-term mean. It results from both an increase of the westerly flow on the south coast of the continent and to the west further north and the northerly flow over land.

[12] Moisture convergence could not be computed from the PCM archive, but the consequences of the perturbation of the flow can be seen in the low level specific humidity and the vertical velocity, which is lower over SWA in FFL. Both fields contribute to the rainfall changes. The consequence of these changes is a reduction of the model total rainfall across most of SWA (Figure 3d). The difference is plotted over the 41 years from 1958 to 1998, however it widens with time. In FFL, across the observation network, the rainfall is 3.5% lower in FF during the 20 years prior to 1977, increasing to 10.8% during the following two decades, which is also when the model response to the FF starts to accelerate [*Meehl et al.*, 2004]. Therefore, although there is a component of the rainfall decline which can be solely attributable to land clearance alone (as suggested by PI04) and there is a component attributable to anthropogenic atmospheric forcing alone (TI06), the combination of FF and land cover changes leads to a larger decline.

[13] The mechanism suggested by PI04 is consistent with our findings, although without a complete moisture balance it is impossible to rule out other mechanisms such as the impact of reduced Leaf Area Index (LAI) on the evapotranspiration which could be responsible for part of the low level humidity response. The interest of this study is to show similar results in a different modelling framework where external forcings other than land clearance are considered and within a fully coupled climate model, avoiding issues related to the impact of boundary conditions. However, the spatial extent of the anomalies differs; this was expected since the model used here has a resolution of about 280 km, while PI04 used regional climate models with resolution of the order of 50 km.

6. Conclusion

[14] Overall, we found that land cover changes appear to have contributed to the rainfall decline in SWA when compared to TI06. We used simulations from a CGCM driven by 20th century atmospheric forcings and compared experiments with two different vegetation cover data sets. The trends obtained using downscaled rainfall are much larger in the experiment where the vegetation has been reduced to grass and crop. The difference in downscaled rainfall between the two sets of experiments is driven by differences in large-scale rainfall while the other large-scale predictor, MSLP, which was found earlier (TI06) to be critical to attribute the rainfall decline to anthropogenic atmospheric forcings does not play an important role in the rainfall response to land clearance. The reduced vegetation cover appears to interact with the changes driven by large-scale circulation to enhance the rainfall trend. Interestingly, this result is found in the statistically downscaled rainfall as well as the direct model rainfall. A strengthening of the wind on the edge of the continent most likely due to the reduced roughness length and reduced moisture above the traditional area of maximal rainfall, is apparent in the three lower levels of the FFL experiment, in agreement with the mechanism described by PI04.

[15] On the balance of evidence, the rainfall decline in SWA that is attributable to anthropogenic atmospheric forcing (TI06) is likely to have been enhanced by the large-scale land clearance which occurred in SWA over the 20th century. However the magnitude of the enhancement must be treated with caution. Firstly it is a model response from a single simulation and secondly the effective land clearance in our simulation is about 4 times what was observed. Despite these legitimate uncertainties, the credibility of this result is reinforced by its consistency with a previous study (PI04). This should encourage further studies with a more realistic land clearance (magnitude and timing).

[16] **Acknowledgments.** Thanks are due to the NCAR Climate Change Research Group for making results from the PCM model available. The IMAGE land cover data set was adapted for the PCM by J. Feddema. The first author is supported by a grant from the Australian Greenhouse Office. Portions of this study were supported by the Office of Biological and Environmental Research, U.S. Department of Energy, as part of its Climate Change Prediction Program and the National Science Fundation.

References

Alcamo, J. (Ed.) (1994), *IMAGE 2.0: Integrated Modeling of Global Climate Change*, 318 pp., Springer, New York.

Allan, R. J., and M. R. Haylock (1993), Circulation features associated with the winter rainfall decrease in southwestern Australia, *J. Clim.*, *6*, 1356–1367.

Australian Surveying and Land Information Group (1990), *Atlas of Australian Resources*, vol. 6, *Vegetation*, 64 pp., Canberra, ACT.

Bonan, G. B. (1996), A land surface model (LSM version 1) for ecological, hydrological and atmospheric studies: Technical description and user's guide, *NCAR Tech. Note NCAR/TN-417+STR*, 150 pp., Natl. Cent. for Atmos. Res., Boulder, Colo.

Cai, W., G. Shi, and Y. Li (2005), Multidecadal fluctuations of winter rainfall over southwest Western Australia simulated in the CSIRO Mark 3 coupled model, *Geophys. Res. Lett.*, *32*, L12701, doi:10.1029/2005GL022712.

Feddema, J., K. Oleson, G. Bonan, L. Mearns, W. Washington, G. Meehl, and D. Nychka (2005), A comparison of a GCM response to historical anthropogenic land cover change and model sensitivity to uncertainty in present-day land cover representations, *Clim. Dyn.*, *25*, 581–610.

Hope, P. (2006), Projected future changes in synoptic systems influencing south west Western Australia, *Clim. Dyn.*, doi:10.1007/S00382-006-0116-x.

Indian Ocean Climate Initiative Panel (IOCI) (2002), Climate variability and change in south west Western Australia, Technical Report, 34 pp., Perth, Australia.

Lyons, T. J. (2002), Cloud prefer native vegetation, *Meteorol. Atmos. Phys.*, *80*, 131–140, doi:10.1007/s007030200020.

Meehl, G. A., W. M. Washington, C. M. Ammann, J. M. Arblaster, T. Wigley, and C. Tebaldi (2004), Combinations of natural and anthropogenic forcings in twentieth-century climate, *J. Clim.*, *17*, 3721–3727.

Pitman, A. J., G. T. Narisma, R. A. Pielke Sr., and N. J. Holbrook (2004), Impact of land cover change on the climate of southwest Western Australia, *J. Geophys. Res.*, *109*, D18109, doi:10.1029/2003JD004347.

Timbal, B. (2004), Southwest Australia past and future rainfall trends, *Clim. Res.*, *26*, 233–249.

Timbal, B., J. M. Arblaster, and S. P. Power (2006), Attribution of the late 20th century rainfall decline in Southwest Australia, *J. Clim.*, in press.

Washington, W. M., et al. (2000), Parallel climate model (PCM) control and transient simulations, *Clim. Dyn.*, *16*, 755–774.

Williams, M. (2003), *Deforesting the Earth: From Prehistory to Global Crisis*, 689 pp., Univ. of Chicago Press, Chicago, Ill.

B. Timbal and J. M. Arblaster, Bureau of Meteorology Research Centre, P.O. Box 1636, Melbourne, Vic 3001, Australia. (b.timbal@bom.gov.au)